A&A 418, 67–75 (2004)
DOI: 10.1051/0004-6361:20040036

Astronomy & Astrophysics

Space distribution of IRAS sources: Difference between oxygen-rich and carbon stars

K. Noguchi, W. Aoki, and S. Kawanomoto

National Astronomical Observatory of Japan, Mitaka, Tokyo 181-8588, Japan

Received 5 February 1998 / Accepted 14 January 2004

Abstract. We have examined the space distribution of IRAS sources in the Galaxy paying attention in particular to the difference between oxygen-rich and carbon stars. The sample consists of about 70 000 sources with good quality photometric data both at 12 and 25 μm. Sample sources are mostly post main sequence stars. Oxygen-rich asymptotic giant branch stars show the highest stellar density at the Galactic center. The density decreases with the increase in the Galactocentric distance. On the other hand, carbon stars show a uniform density distribution within about 3.6 kpc of the Sun. Thus the ratio of carbon stars to oxygen-rich asymptotic giant branch stars increases with the increase in the Galactocentric distance within the range between about 5 and 12 kpc.

Key words. Galaxy: stellar content – Galaxy: structure – infrared: stars – stars: AGB and post-AGB – stars: carbon – stars: late-type

1. Introduction

There are two types of asymptotic giant branch (AGB) stars; oxygen-rich (O-rich) AGB stars and carbon stars. It is generally assumed that ordinary carbon stars are created from O-rich AGB stars when carbon atoms are dredged up from the core by the deep convective envelope developed after a helium shell flash. It is also known that the space distribution of O-rich AGB stars is different from that of carbon stars in the solar neighborhood. The difference in the space distribution between carbon stars and O-rich AGB stars means that the fraction of O-rich AGB stars which evolve into carbon stars varies depending on the location in the Galaxy. The evolutionary process on the AGB is probably affected by various factors. It is interesting to investigate the space distribution of carbon stars extensively and compare it with that of O-rich stars to clarify the cause of the difference in the space distribution.

Blanco (1965) first reported the difference in the space distribution between O-rich stars and carbon stars. He reported that while the stars of type M 2 to M 4 appear to increase in number toward the Galactic Center (GC), carbon stars do not show a preference for the GC. Claussen et al. (1987) examined the space distribution of 215 carbon stars taken from the *Two Micron Sky Survey* (TMSS) (Neugebauer & Leighton 1969). Although their sample is not complete in the range of $-90° < l < 0°$ because of the lack of TMSS for this region, they reported a rather uniform distribution of carbon stars within 1.5 kpc of the Sun. Thronson et al. (1987) examined 619 carbon-rich objects selected within certain color ranges on the two-color diagram based on the IRAS (InfraRed Astronomical Satellite) data. They reported that the number density of carbon-rich objects shows no Galactocentric gradient within about 5 kpc of the Sun despite the remarkable gradient of the number density of O-rich stars. Jura & Kleinmann (1990) also reported that there is no gradient in the space distribution of the 126 very dusty carbon stars within about 2.5 kpc of the Sun. All these works have shown the difference in the distribution between O-rich stars and carbon stars. However, they are based on small samples of carbon stars that cover only fairly limited areas in the Galaxy. It should be noted that the area covered by Thronson et al. (1987) turned out to be much smaller than that estimated by them (see Sect. 4.3).

We have attempted to examine the space distribution of post main sequence (Post-MS) stars as extensively as possible by using IRAS sources paying attention in particular to the difference between carbon stars and O-rich stars. IRAS, launched in 1983, surveyed about 96% of the sky at 12, 25, 60, and 100 μm and reported photometric data of about 250 000 point sources. Approximately 65% of the sources detected are stars (Beichman 1987). The majority of these stars are in the stage of Post-MS evolution. Since it is required to analyze as many stars as possible for better statistics and to reach as large a radius of space as possible, we selected IRAS sources with good quality photometric data both at 12 and 25 μm. The number of such sources is 71 567. We found correlation between [12]−[25] and the characteristics in

Send offprint requests to: K. Noguchi,
e-mail: knoguchi@optik.mtk.nao.ac.jp

the low resolution spectra (LRS), and used [12]−[25] as an indicator of the characteristics of sources ([12] and [25] are mean magnitudes at 12 and 25 μm, respectively).

The relation between [12]−[25] and the LRS characteristics is discussed in Sect. 2. The Galactic longitude distribution of sources is examined in Sect. 3. It is shown in Sect. 3 that IRAS sources are divided into two groups of sources with different longitude distributions. In Sect. 4, the space distribution of sources projected onto the Galactic plane is derived by estimating the distances of sources. The distribution of carbon stars is compared with that of O-rich stars in Sect. 4. In Sect. 5, we discuss our results by correlating with the metallicity.

2. Correlation between LRS characteristics and infrared color

In this section we discuss the correlation between the LRS characteristics and [12]−[25] to make a scale to classify IRAS sources without the LRS data on the basis of [12]−[25].

IRAS Science Team (1986) reported the LRS for 5425 bright sources (the LRS sources). The LRS sources can be divided into groups of sources with different spectral characteristics.

We classified the LRS sources into 7 groups on the basis of the Automatic Classification (Cheeseman et al. 1989). Cheeseman et al. (1989) classified the LRS into 9 classes (α, β, γ, δ, ϵ, ζ, η, θ, and λ class) and further divided into subclasses, and described source counts, source types, and the spectral quality for respective subclasses in their catalogue. Subclasses and θ class containing only sources with noisy spectra are rejected from the present analysis. The η and ζ classes are united as one group, because sources in both classes are similarly characterized by the 10-μm silicate absorption feature. Other autoclasses are adopted as individual groups. Accordingly we divided the LRS sources into 7 groups. The numbers of sources for respective groups are shown in Fig. 1 by 7 line graphs as functions of [12]−[25]. Magnitudes at 12 and 25 μm are calculated on the basis of the 0-mag fluxes of 28.3 and 6.73 Jy at respective bands. Magnitudes are not color corrected. The total number of sources is 3433.

Characteristics of respective groups are described briefly in the following. Most O-rich stars are classified into the following 4 groups. Carbon stars are rare in these groups.

– 1: δ class; The LRS are featureless. Sources in this group are almost free of circumstellar dust emission.
– 2: β class; The LRS show silicate emission features at 10 and 18 μm. Sources in this group are generally surrounded by optically thin circumstellar dust envelopes (CDEs).
– 3: ϵ class; The LRS show silicate emission features superposed on some self-absorption. Sources in this group are associated with CDEs with medium optical thickness.
– 4: η-ζ class; The LRS show a silicate absorption feature at 10 μm. These sources are surrounded by optically thick CDEs.

While there is a gap between the mean [12]−[25] value of the δ-class sources and that of the β-class sources, the β, ϵ,

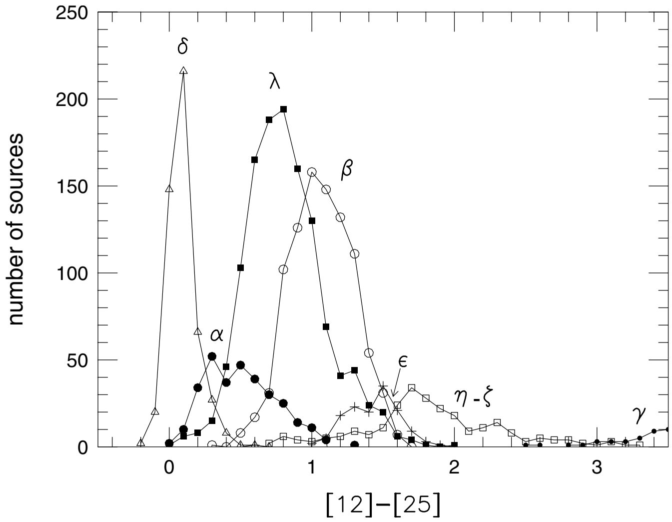

Fig. 1. The number of sources vs. [12]−[25] for 7 groups of the LRS sources. Each group is classified on the basis of the Automatic Classification by Cheeseman et al. (1989). Sources in subclasses with the noisy LRS in the Automatic Classification are not included in the figure. The number of sources is plotted for each 0.1 mag interval in [12]−[25].

and the η-ζ classes form a continuous sequence with increasing [12]−[25] corresponding to the increase in the optical thickness of CDEs.

The fifth group contains λ-class sources which generally show featureless spectra or weak emission features. This group is a mixture of O-rich stars and carbon stars, but the majority are O-rich stars. The λ-class sources have slightly smaller [12]−[25] values on average than those of the β-class sources (Fig. 1).

Carbon stars are usually classified into the α class characterized by the 11.3-μm SiC emission feature. The mean [12]−[25] value of this group is between those of the δ class and the β class. No O-rich star is identified in this group.

Both planetary nebulae and HII regions are generally included in the γ class, which has the largest [12]−[25] value ([12]−[25] $\geq$ 3 mag).

Although it is difficult to classify sources into 7 groups using only [12]−[25] because of the overlaps of respective [12]−[25] ranges, [12]−[25] can be an indicator of source types. Assuming that the relation between the LRS characteristics and [12]−[25] is applicable also for fainter IRAS sources without good quality LRS data, we use [12]−[25] as an indicator of source characteristics instead of LRS data.

3. Galactic longitude distribution

In this section we discuss the Galactic longitude distribution of IRAS sources. IRAS sources with good quality photometric data both at 12 and 25 μm were selected as the sample. For sources with good quality data also at 60 μm, the sources with [12]−[60] > 4 mag were rejected (4284 sources) because most of them are not stars (Noguchi et al. 1993). The total number of sources selected in this way is 67 283.

3.1. Longitude distribution of IRAS sources

The longitude distribution of sources is examined for 4 groups of IRAS sources divided on the basis of the value of [12]−[25]. The 4 groups are sources with [12]−[25] < 0.5 mag, 0.5 ≤ [12]−[25] < 1.2 mag, 1.2 ≤ [12]−[25] < 1.6 mag, and 1.6 ≤ [12]−[25] < 3 mag, respectively. While the latter 3 groups mostly consist of O-rich stars with increasing optical thickness of the CDEs with the increase in [12]−[25], the first group contains different kinds of sources from the latter 3 groups as discussed in Sect. 3.3. The distribution of sources on the l–b plane (l–b distribution) is shown in Fig. 2 for these 4 groups. While all the 3 groups of sources with [12]−[25] ≥ 0.5 mag (hereafter referred to as red sources) show a density maximum in the GC direction, sources with [12]−[25] < 0.5 mag (hereafter referred to as blue sources) show a different longitude distribution from those of the other 3 groups. We discuss the distributions of red sources and blue sources separately in the following subsections.

3.2. Red sources

The red sources contain the β-, ϵ-, η-, ζ-, and λ-class sources as shown in Fig. 1. Although a part of α-class sources (carbon stars) are also included, red sources are mostly O-rich AGB stars with CDEs. Thus l–b distributions of red sources in Figs. 2b−d reflect the distribution of O-rich AGB stars with the increasing optical thickness of CDEs from Figs. 2b to 2c and then to 2d. Since the Galactic bulge is clearly seen in Fig. 2d, sources in Fig. 2d are detected up to the distance of the GC or farther. However, most sources with 0.5 ≤ [12]−[25] < 1.2 mag (Fig. 2b) are probably located nearer than the GC because the sources are distributed in a rather wide latitude region.

3.3. Blue sources

Blue sources show a different longitude distribution from that of red ones. They do not show the density maximum in the GC direction. We discuss what kind of component stars contribute to the blue sources and what longitude distributions the respective components have.

The LRS sources with [12]−[25] < 0.5 mag consist of the δ-, α-, λ-, and β-class sources. The mean values of [12]−[25] for the δ-, α-, λ-, and β-class sources increase in this order as shown in Fig. 1. We examine the l–b distributions of components of blue sources by dividing them into small groups on the basis of the value of [12]−[25]. In this process we expect that bluer sources (e.g. [12]−[25] < 0.2 mag) correspond to the δ class while redder sources (e.g. [12]−[25] > 0.4 mag) correspond to the λ or β class. The sources with an intermediate color (e.g. [12]−[25] ∼ 0.3 mag) are expected to correspond to the α class.

Another useful method for decomposing the sources is the count of sources against the apparent magnitude. The number of sources within a certain distance of the Sun (r) increases with the r^3 dependence within the thickness of the Galactic disk. On the other hand, the number increases with the r^2 dependence at

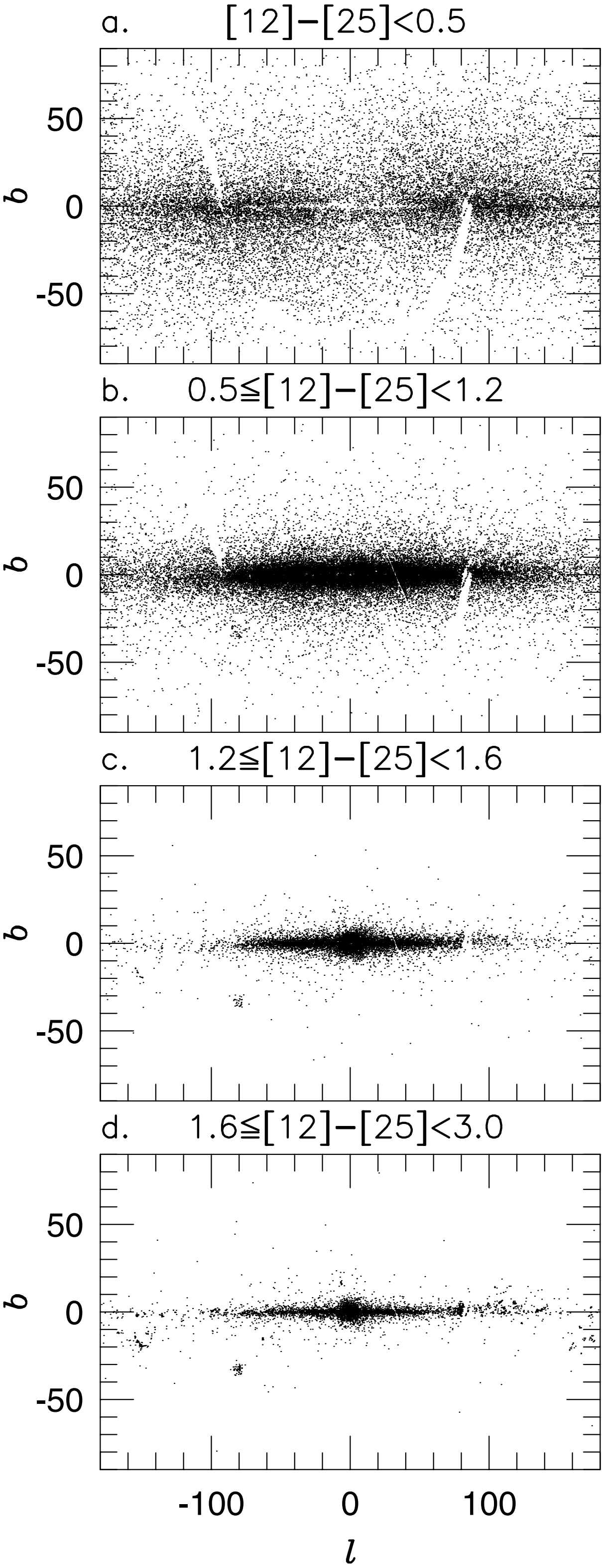

Fig. 2. a)–d) l–b distributions for 4 color ranges of sample sources. A band-shaped low-density area is seen in Fig. 2a along the Galactic plane centered on the GC. This is probably due to an observational effect caused by source confusion. Longitude axis is plotted backwards in this figure compared with ordinary ones. Thus the source cluster in the lower left quadrant at (l, b) ≃ (−80°, −33°) corresponds to the Large Magellanic Cloud.

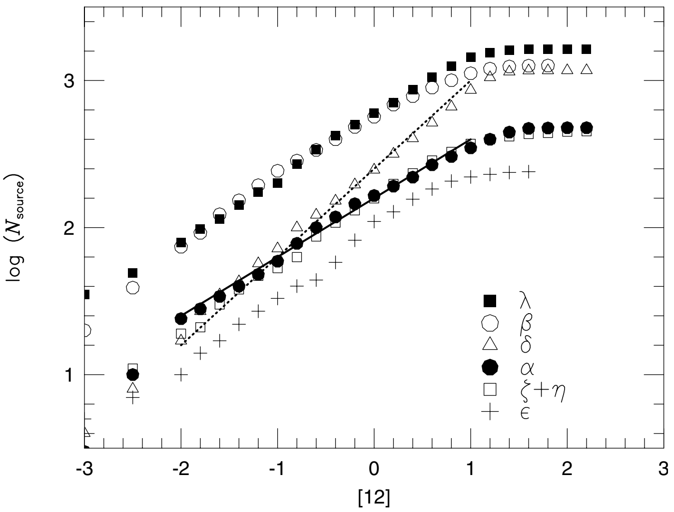

Fig. 3. Number of sources brighter than a given magnitude at 12 μm vs. [12] for the LRS sources. Sources are shown separately for individual source types. Solid and dotted lines correspond to the relation of $N \propto r^2$ and $N \propto r^3$, respectively, in which r is the distance from the Sun.

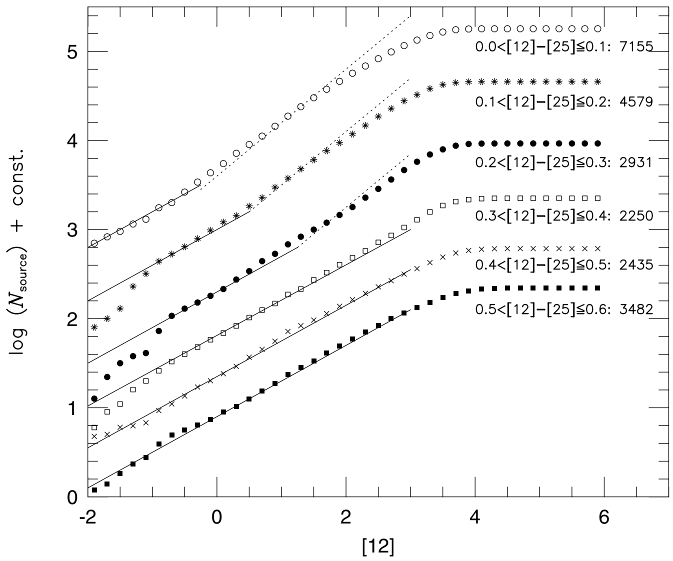

Fig. 4. Number of sources brighter than a given magnitude at 12 μm vs. [12] for our sample sources for respective 0.1 mag intervals in [12]−[25]. The [12]−[25] range and the total number of sources in each interval are given in the figure. The definition of the slant lines is the same as that in Fig. 3.

distances much farther than the thickness of the Galactic disk. Such a difference of the r dependence is an indicator that distinguishes between nearby sources and distant ones. In this context the thickness of the Galactic disk is a typical scale to distinguish the two sources. To check this presumption, the number of sources brighter than a given magnitude at 12 μm for the LRS sources is shown in Fig. 3. Only the δ-class sources are well fitted by the r^3 dependence in the range of [12] < 1 mag instead of the r^2 dependence which is suitable for other classes of sources. Thus the δ-class sources are mostly nearby stars. Since the δ-class sources identified with visible sources are dominated by K- or (early) M-type giants, the r^3 dependence reflects the distribution of nearby late-type giants. On the other hand, the r^2 dependence suitable for other classes means that we are observing sources distributed up to the distances farther than the thickness of the Galactic disk.

Figure 4 shows a diagram similar to Fig. 3 but for our sample including sources without LRS. The diagram is made for sources within individual 0.1 mag intervals of [12]−[25]. It is important to note that these sources are likely to be detected completely in the range of [12] ≤ 3 mag. In this range the slope is gradually changing depending on [12]−[25]. The slope is steeper than the r^2 dependence in a certain [12] range for each group of sources in cases of [12]−[25] ≤ 0.3 mag. This means that the sources in this [12]−[25] range are the mixture of two components of sources, one of which shows r^2 dependence and the other of which shows an r^3 dependence. The [12] range with steep slope is wider for groups with smaller [12]−[25] values. This result is consistent with the fact that the δ-class sources dominate in bluer sources ([12]−[25] ≤ 0.2 mag). On the other hand, the slope is well approximated by the r^2 dependence for groups with [12]−[25] > 0.3 mag, accordingly distant sources dominate in these groups. It would be good to quantify what "nearby" and "distant" mean in this context. Given a scale height of 270 pc for K-type giants (Wainscoat et al. 1992), for example, we would assume that nearby means sources within 300 pc to 600 pc of the Sun. For K4,5 (or M 3) giants with the absolute magnitude at 12 μm of −3.26 (or −5.51) (Wainscoat et al. 1992) and a completeness limit of [12] < 3 mag the detection radius would be about 180 pc (or 500 pc).

What kind of sources are dominant in the range of 0.3 < [12]−[25] ≤ 0.4 mag? We examined the associations for LRS sources in this color range. 54% of the sources are α-class sources or identified with carbon stars in *A General Catalogue of Cool Galactic Carbon Stars, Second Edition* (GCCS2; Stephenson 1989) and 34% are identified with O-rich stars. If the fraction of carbon stars in this color-range of sample sources is similar to that of LRS sources with the similar color, it is probably about 60%. Since the number count of sources against [12] fits r^2 dependence rather well in this color range as shown in Fig. 4, the contribution of the δ-class sources, which show r^3 dependence, is expected to be minor. On the basis of the above analysis, we concluded that the sources with 0.3 < [12]−[25] ≤ 0.4 mag exhibit the distribution of carbon stars.

Summarizing the above discussion, we classify blue sources into 4 groups :

– 1: sources with [12]−[25] ≤ 0.2 mag (11 734 sources); most sources are nearby K- or M-giants;
– 2: sources with 0.2 < [12]−[25] ≤ 0.3 mag (2931); these are the mixture of nearby giants and carbon stars;
– 3: sources with 0.3 < [12]−[25] ≤ 0.4 mag (2250); carbon stars are dominant;
– 4: sources with 0.4 < [12]−[25] ≤ 0.5 mag (2435); O-rich AGB stars are dominant.

The l–b distributions of blue sources are shown in Fig. 5 for respective [12]−[25] ranges separately. Since our sample is almost complete within the range of [12] ≤ 3 mag, only sources in this range are shown in Fig. 5. While longitude dependence is almost flat for sources in the range of [12]−[25] ≤ 0.4 mag, source density is highest in the GC direction for sources in the range of [12]−[25] > 0.4 mag. Although the distributions in Figs. 5a−d all show almost flat longitude dependence, the latitude distribution varies depending on [12]−[25]. It should be noted that the distribution of carbon stars (0.3 < [12]−[25] ≤ 0.4 mag: Fig. 5d) is characterized by the concentration towards the Galactic plane, which can not be seen for nearby stars, with almost flat longitude dependence.

Although Fig. 2a shows the deficiency of sources in the GC direction, the distribution of the sources in Fig. 5 does not show such a tendency. The difference is due to the contribution of faint sources with [12] > 3 mag in Fig. 2a. This is due to source confusion effects as IRAS scanned across the Galactic plane.

3.4. Two types of longitude distribution

We found that the density of O-rich AGB stars shows strong longitude dependence. The density is highest in the GC direction and decreases toward the anti-center direction. On the other hand, there is another type of source that shows almost flat longitude dependence. The latter sources can be divided further into two groups. One is the group of nearby stars which is distributed in the wide latitude range, and the other is the group of sources dominated by carbon stars which is distributed in the relatively narrow latitude range. Thus we conclude that the longitude distribution of carbon stars is different from that of O-rich AGB stars.

To investigate the difference in the actual space distribution, distance estimation for individual sources is essential. We try to estimate distances of our sample in the next section.

4. Space distribution of IRAS sources

4.1. Projection onto the Galactic plane: O-rich AGB stars

In Sect. 3, the source distribution was discussed on the l–b plane. In this section, we examine the space distribution of sources projected onto the Galactic plane by estimating distances of sources. Our discussion starts from how distances are evaluated.

IRAS sources with good quality photometric data both at 12 and 25 μm are generally detected within the faintest limit of about 4.5 and 3.3 mag at 12 and 25 μm, respectively. The diagram of [12] vs. [12]−[25] for sources within $-10° < l \leq 10°$ and $|b| \leq 10°$ (GC direction) is shown in Fig. 6 with lines corresponding to these magnitude limits. The sample is almost complete in the range of [12] ≤ 3 mag as discussed in Sect. 3.3.

For a certain narrow color range of sources, i.e. for similar types of sources, observed [12] values can be an indicator of distances if the luminosity of sources is the same. When we choose sources with [12]−[25] ≃ 2 mag in Fig. 6, the source density changes depending on [12] with the maximum at [12] ≃ 2.5 mag. Since 2.5 mag is brighter than the completeness limit ([12] ≃ 3 mag), the density maximum should be real. Since the

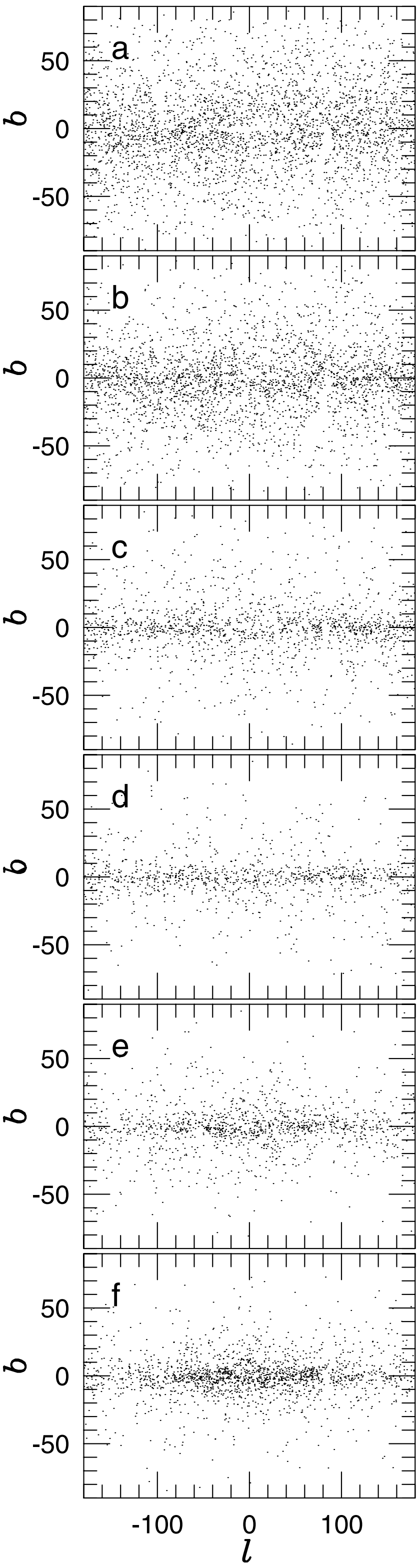

Fig. 5. a)–f) l–b distributions of sample sources for individual 0.1 mag intervals of [12]−[25]. Only bright sources with [12] ≤ 3.0 mag are shown. The following [12]−[25] ranges correspond to respective figures: **a)** 0 < [12]−[25] ≤ 0.1 mag, **b)** 0.1 < [12]−[25] ≤ 0.2 mag, **c)** 0.2 < [12]−[25] ≤ 0.3 mag, **d)** 0.3 < [12]−[25] ≤ 0.4 mag, **e)** 0.4 < [12]−[25] ≤ 0.5 mag, **f)** 0.5 < [12]−[25] ≤ 0.6 mag.

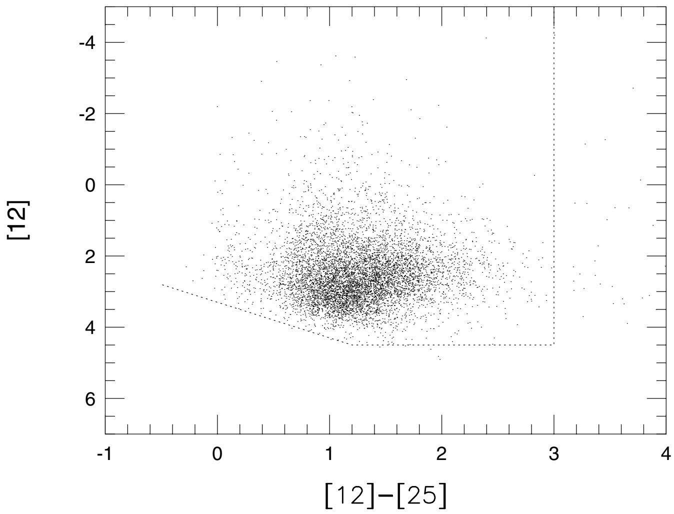

Fig. 6. [12] vs. [12]−[25] for sample sources near the GC ($-10° < l \leq 10°$ and $|b| \leq 10°$). Detection limits roughly estimated ([12] = 4.5 mag, [25] = 3.3 mag) are shown with dashed lines. Since sources with [12]−[25] ≤ 3 mag are discussed in this paper, this border is also shown.

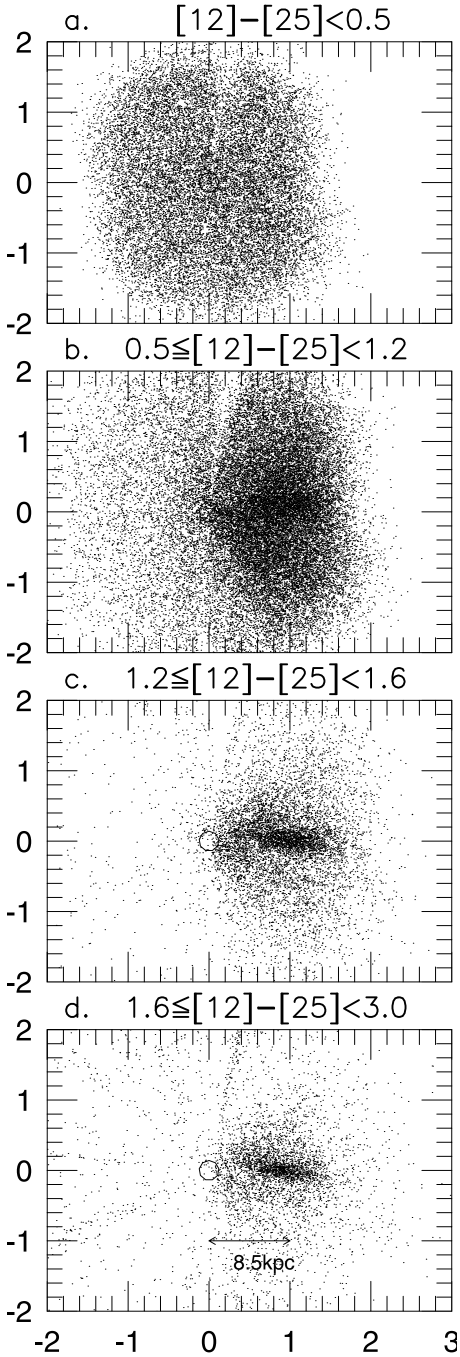

Fig. 7. a)–d) Projection of the sample sources onto the Galactic plane viewed from the north pole. Sources are divided into 4 groups with different color ranges. The location of the Sun is shown with a circle at (0, 0) position. The distance scale is given as that from the Sun by assuming that all the sources have the same absolute magnitude (−12.1 mag) at 12 μm. The GC is to the right from the Sun. In Fig. 7d, (1, 0) point corresponds to the GC. However, in Figs. 7a–c, (1, 0) points are nearer than the GC because the actual absolute magnitude is fainter than −12.1 mag at 12 μm in these color ranges (see the text).

Galactic bulge is clearly seen in Fig. 2d, the sample sources with 1.6 ≤ [12]−[25] < 3.0 mag are probably detected up to the distance of the GC. Accordingly we identify this maximum density at [12] ≃ 2.5 mag with the highest stellar density at the GC. Habing et al. (1985) have discussed the stars in the bulge of the Galaxy detected by IRAS. They reported that the mean 12 μm flux density of the sources defining the bulge is about 2.3 Jy ([12] = 2.73 mag) within the color range of 1.12 < [12]−[25] < 2.31 mag. Thus our assumption of the magnitude at 12 μm at the GC ([12] = 2.5 mag) is 0.23 mag brighter than the value by Habing et al. (1985) but the difference is not large.

On the basis of the above assumption, we obtain the mean magnitude of IRAS sources with [12]−[25] = 2 mag to be 2.5 mag at 12 μm when they are at the GC. The 2.5 mag at the GC (8.5 kpc from the Sun) corresponds to the absolute magnitude of −12.1 mag.

By using this mean absolute magnitude at 12 μm, we calculate distances of individual sources by comparing them with apparent magnitudes. Since the luminosity and the fraction of the energy radiated at 12 μm both depend on the color of sources, the absolute magnitude assumed at 12 μm depends on [12]−[25]. However, we assume that −12.1 mag is applicable for sources with [12]−[25] > 1.6 mag because the density maximum in Fig. 6 appears to be at [12] ≃ 2.5 mag in this color range. We also assume that −12.1 mag is applicable both for bulge and disk stars. With the reluctant assumption of a monochromatic luminosity for all the sources in this color range, the estimated statistical distances include inevitable errors. This is the main uncertainty in our analysis which distorts the actual space distribution.

We tentatively evaluate the distances of all the sample sources by assuming the absolute magnitude at 12 μm to be −12.1 mag also for sources with [12]−[25] ≤ 1.6 mag, and derive the source distribution in the Galaxy for comparison. The obtained space distributions projected onto the Galactic plane are shown in Fig. 7 for 4 groups of sources with respective [12]−[25] ranges, where the distances on the Galactic plane are normalized to 8.5 kpc. It should be noted that the distance scales in Figs. 7a–c are not correct because the mean absolute magnitudes of sources in this color range should be fainter than −12.1 mag at 12 μm. Therefore, we do not use the scales as actual ones in the range of [12]−[25] ≤ 1.6 mag.

Although our distance estimation includes uncertainties mainly due to the assumption of monochromatic luminosity, sources with 1.6 ≤ [12]−[25] < 3.0 mag show the clear concentration surrounding the GC as shown in Fig. 7d. Although the high source density area in Fig. 7d is elongated along the radial direction from the Sun, this elongation is not real but is probably due to the dispersion of the absolute magnitudes of individual sources. Despite the difference of the distance scale, all the distributions in Figs. 7b–d are interpreted as similar ones showing the highest source density at the GC and we are detecting sources with increasing depth from the Sun in the order from Figs. 7b to 7c and then to 7d. These distributions reflect the space distribution of O-rich AGB stars.

Although the actual distance scale is not evaluated, the source distribution in Fig. 7a appears to be different from those in Figs. 7b–d as expected from the difference in the longitude distribution discussed in Sects. 3.2 and 3.3.

4.2. Uniform distribution of carbon stars

As discussed in Sect. 3.3, we propose that the distribution of sources with 0.3 < [12]−[25] ≤ 0.4 mag reflects that of carbon stars. To compare the distribution of carbon stars with that of O-rich AGB stars, we evaluate the distances of sources in this color range by assuming a monochromatic luminosity again. Distances are estimated in the following way. First, total radiant energies (TREs) observed are estimated. Second, distances are calculated by comparing TREs with the luminosity assumed for carbon stars.

The TREs are estimated by using the IRAS data at 12 μm and a simple model spectrum. The model spectrum was made as a smooth curve which fits well the spectral energy distributions (SEDs) of carbon stars with 0.3 < [12]−[25] ≤ 0.4 mag. The SEDs are based on the near-infrared (NIR) photometric data (Noguchi et al. 1981, 1991) and IRAS data. Since flux maxima of carbon stars with 0.3 < [12]−[25] ≤ 0.4 mag are mostly at the wavelengths of about 1.5 μm on the diagram of λF_λ vs. λ, TREs (W/cm^2) are evaluated by assuming that all these sources have flux maxima at 1.5 μm. The assumed model spectrum is rather similar to the blackbody spectrum with a temperature of about 2000 K. But our model spectrum gives 23% larger TREs for a given 12 μm fluxes than those based on the blackbody spectrum. Thus the calculated distances based on our model spectrum give about 11% smaller values than those when based on the blackbody spectrum. The TREs (W/cm^2) and the 12 μm fluxes (λF_λ : W/cm^2) are correlated as follows: TRE = 38 $\lambda F_\lambda(12\,\mu\mathrm{m})$.

Mikami (1975) has evaluated the bolometric magnitude ($M_{\rm bol}$) of N-type carbon stars to be −5.23 mag, corresponding to 10 000 $L_\odot$. Groenewegen et al. (1992) have assumed $M_{\rm bol}$ = −4.9 mag (L = 7070 $L_\odot$) to derive distances of carbon stars. Jura & Kleinmann (1990) and Guglielmo et al. (1993) have adopted 10 000 $L_\odot$ for carbon stars with high mass loss. Among these works carbon star luminosity is estimated or assumed in the range between 7000 $L_\odot$ and 10 000 $L_\odot$.

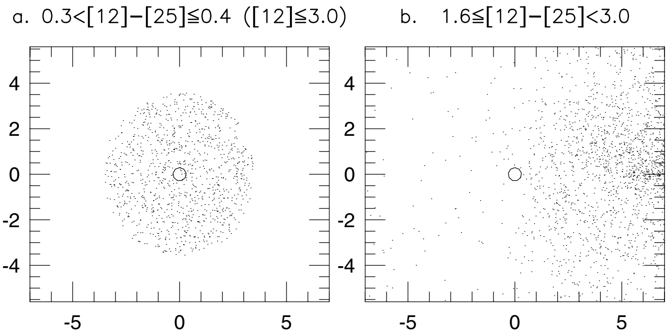

Fig. 8. a) Projection of sample sources with 0.3 < [12]−[25] ≤ 0.4 mag onto the Galactic plane viewed from the north pole. The location of the Sun is shown with a circle at (0, 0) position. Distances are given in kpc from the Sun. The GC is to the right from the Sun. The distance scale is estimated by assuming the luminosity of carbon stars to be 7000 $L_\odot$. **b)** Projection of sample sources with 1.6 ≤ [12]−[25] < 3.0 mag.

We assume 7000 $L_\odot$ for our distance estimation. This luminosity corresponds to the absolute magnitude of −9.8 mag at 12 μm when based on our model spectrum.

The space distribution projected onto the Galactic plane is shown in Fig. 8a for sources which satisfy both 0.3 < [12]−[25] ≤ 0.4 mag and [12] ≤ 3 mag. These sources are distributed uniformly within the area about 3.6 kpc of the Sun. If interstellar extinction ($A_{\rm v}$) is 1 mag/kpc within 3.6 kpc of the Sun, the distance limit still reaches 3.4 kpc when we assume the extinction at 12 μm is 0.037 $A_{\rm v}$ (Rieke & Lebofsky 1985). Although the distance limit of 3.6 kpc may not be very accurate, the area is likely to reach at least 3 kpc from the Sun. On the other hand, the distance limit probably does not reach the GC, because about 40 000 $L_\odot$ is required for carbon star luminosity to reach the GC even if we neglect the interstellar extinction. Thus the distribution of carbon stars near the GC is not clarified by the present analysis. In Fig. 8b we show the case of O-rich AGB stars in Fig. 7d again with the same scale as that in Fig. 8a for comparison. Since O-rich AGB stars show a clear density increase toward the GC, we conclude that the space distribution of carbon stars is quite different from that of O-rich AGB stars within a radius of 3.6 kpc from the Sun.

The space density of carbon stars projected onto the Galactic plane can be estimated on the basis of our results. By assuming that 60% of 2250 IRAS sources with 0.3 < [12]−[25] ≤ 0.4 mag are carbon stars distributed within radius of 3.6 kpc from the sun, the projected space density is evaluated to be 33 stars/kpc^2. However this value should be a lower limit because many carbon stars are outside this color range. We try to estimate the total space density of all carbon stars based on the ratio of carbon stars within the range of 0.3 < [12]−[25] ≤ 0.4 mag to those outside this range in two ways using two different groups of carbon stars. One is based on LRS sources classified into the α-class. There are 476 α-class sources with good quality photometric data both at 12 and 25 μm. Among them, 60 stars are in the range of 0.3 < [12]−[25] ≤ 0.4 mag. By using this ratio the space density of all carbon stars is estimated to be 263 stars/kpc^2. Here all the α-class sources are assumed to have the same absolute magnitude at 12 μm. This value also should be a lower limit because some carbon stars are classified into classes other than α class (e.g. λ class). The other method is based on carbon stars in GCCS2. Among 5987 carbon stars listed in GCCS2, 2032 stars are identified as IRAS sources with good quality photometric data both at 12 and 25 μm and 400 stars are within the range of $0.3 < [12]-[25] \leq 0.4$ mag. The total space density of carbon stars is estimated to be 168 stars/kpc^2 by extrapolating on the basis of carbon stars in GCCS2. Since most of the carbon stars in GCCS2 are identified based on optical spectra, red carbon stars are not complete. Thus 168 stars/kpc^2 is also a lower limit. Since the process to extrapolate to the total space density of all carbon stars contains a large uncertainty, the discrepancy between two values estimated based on two different samples is fairly large. However, the total space density of all carbon stars is likely to be much higher than that estimated by Claussen et al. (1987) (43 stars/kpc^2) or Thronson et al. (1987) (38 stars/kpc^2).

4.3. Comparison with other works

It is already known that carbon stars show rather uniform space distribution in the solar neighborhood. Papers reported by Claussen et al. (1987), Thronson et al. (1987), and Jura & Kleinmann (1990) report the space distribution of relatively bright carbon stars. In this section we compare our result with those reported in these papers. All or most of the sample stars in these papers are true carbon stars, while our sample may include about 40% contamination. All the sample stars in the paper by Claussen et al. (1987) are visually identified true carbon stars and those of Thronson et al. (1987) are estimated to contain only about 7% contamination. Sources of Jura & Kleinmann (1990) are mostly carbon stars with spectroscopic evidence.

Claussen et al. (1987) reported that carbon stars show a uniform distribution within about 1.5 kpc of the Sun. They evaluated the distances of 215 carbon stars in the TMSS by assuming that the absolute magnitude of all their sample stars is -8.1 mag at K band. Most of their stars show similar colors to those of our samples. If we assume our model spectrum of carbon stars for their samples, -8.1 mag at K corresponds to the luminosity of 8800 $L_{\odot}$. Thus their distances are systematically 1.12 times larger than our estimation. Therefore, our distance limit is about 2.7 times larger than that by Claussen et al. (1987).

Thronson et al. (1987) examined the distribution of 619 carbon-rich objects in the Galaxy. Their sample is selected from IRAS sources with good quality photometric data at 12, 25, and 60 μm. Their sample is in certain color ranges on the two-color diagram ($-0.09 \leq [12]-[25] \leq 0.61$ mag and $0.18 \leq [25]-[60] \leq 1.88$ mag), where sources are mostly carbon stars. Although the median of their [12]−[25] range (0.26 mag) is a little smaller than that of our sample (0.35 mag), the majority of their sample sources are in the color range similar to that of our sample. They reported that their carbon-rich objects are distributed uniformly in the Galaxy up to the distance of about 5 kpc from the Sun by assuming that all their sources have the same luminosity at 12 μm ($L_{12} = 3 \times 10^9$ Jy pc^2). However, their distance limit should be considerably overestimated. If we estimate their luminosity by using our model spectrum with the flux maximum at 1.5 μm, it corresponds to about 70 000 $L_{\odot}$, which is the absolute magnitude of -12.3 mag at 12 μm. This luminosity should be too high for the typical luminosity of carbon stars. If we assume 7000 $L_{\odot}$ for their sample sources to compare their distance scale with ours, their distance limit is about 1.6 kpc from the Sun. Accordingly our distance limit is about 2.2 times larger than that by Thronson et al. (1987).

Thus, the present work demonstrates the distribution of carbon stars more extensively than the works by Claussen et al. (1987) and Thronson et al. (1987), though our sample includes a rather large amount of contamination.

While the works by Claussen et al. (1987) and Thronson et al. (1987) discussed the space distribution of carbon stars with the similar color to our carbon star sample, Jura & Kleinmann (1990) examined the distribution of 126 very dusty carbon stars. They reported that dusty carbon stars are also distributed uniformly within about 2.5 kpc of the Sun. All their sample stars are very bright at 12 μm ($[12] \leq -0.38$ mag) and most of them (121 stars) are LRS sources. While 51 sources belong to the α class, 64 sources belong to the λ class. Their sources are in the fairly wide color range ($-0.1 < [12]-[25] < 2.5$ mag) among which 106 sources are in the range of $[12]-[25] \geq 0.4$ mag. Thus their sources are mostly redder than our carbon star sample. They estimated distances of sources by comparing the TRE evaluated on the basis of the IRAS 12-μm flux (TRE = $4.1\,\lambda F_{\lambda}(12\,\mu$m)) with an assumed luminosity of 10 000 $L_{\odot}$. Since the color range of their sample is different from that of our sample, it is difficult to compare their distance scale accurately with ours, because both the bolometric correction and the luminosity should be different from ours. It is interesting that very dusty carbon stars also show a uniform space distribution, although the number of their sample is quite limited.

5. Discussion

While the number density of the O-rich AGB stars decreases with the increase in the galactocentric distance (Rg), carbon stars show the uniform distribution projected onto the Galactic plane within the area about 3.6 kpc of the Sun. This suggests that the difference in the space distribution between O-rich AGB stars and carbon stars is not limited only in the solar neighborhood but also on the extensive scale of the Galaxy. The result of this study enables us to discuss the ratio of carbon stars to O-rich AGB stars on the scale of the Galaxy.

The behavior of the ratio of carbon stars to M-type stars (C/M ratio) in M 31 is qualitatively similar to our result. Brewer et al. (1995) have examined the C/M ratio for five fields in M 31 spanning the Rg (M 31) (distance from the center of M 31) from 4 to 32 kpc along the semi-major axis. They reported that the C/M ratio increases smoothly with the Rg (M 31). The similarity between the Galaxy and M 31 indicates that the higher C/M ratio prefers the larger Rg generally among this type of spiral galaxies.

What are the important factors that determine the C/M ratio? The metallicity, especially oxygen abundance, is proposed as a strong candidate because carbon atoms dredged up from the stellar core affect the C/O ratio in the atmosphere more effectively for the atmosphere with less oxygen abundance. Actually, combining data from various external galaxies (LMC, SMC, IC 1613, NGC 55, NGC 300, NGC 6822, M 31, and M 33), Pritchet et al. (1987) reported that the C/M ratio has a correlation with the metallicity, in the sense that higher C/M ratios appear in lower metallicity environments.

The *R*g (M 31) dependence of the C/M ratio in M 31 was compared with that of the metallicity by Brewer et al. (1995). They reported that the metallicity in M 31 decreases smoothly with the increase in the *R*g (M 31) and that the C/M ratio is inversely correlated with the metallicity.

For our Galaxy, Smartt & Rolleston (1997) reported the distribution of oxygen abundance on the basis of the spectroscopic data of early B-type stars and derived the gradient of -0.07 ± 0.01 dex kpc^{-1} within $6 < Rg < 18$ kpc. Rolleston et al. (2000) reported that the abundances of C, N, Mg, Al, and Si also show similar gradients to that of oxygen, indicating the decrease in metallicity with an increase in the *R*g. Thus our result on the ratio of carbon stars to O-rich AGB stars in the Galaxy is also correlated inversely with the metallicity. The anti-correlation between the C/M ratio and the metallicity, which has been proposed as an important factor for deciding the C/M ratio in galaxies, is likely to be applicable also to our Galaxy.

As discussed above, the difference in the space distribution between carbon stars and O-rich AGB stars seems to be explained as due to the metallicity gradient in the Galaxy. However, it is an another interesting question why carbon stars show a uniform distribution in the Galaxy. Is the apparent uniformity of the distribution of carbon stars actually the result of fortuitous cancellation between the stellar density gradient and the metallicity gradient? Whether the uniformity is only the fortuitous result or an essential characteristic to be explained by correlating with the structure and/or the formation of the Galaxy is an important point to be clarified by further works. It is also interesting to clarify whether the carbon stars show a uniform distribution including in the GC region.

6. Conclusions

We have examined the space distribution of about 70 000 IRAS sources in the Galaxy paying attention in particular to the difference between the distribution of carbon stars and that of O-rich AGB stars. The longitude distribution of sources were examined by dividing sources into those with individual [12]−[25] ranges. Sources with $1.6 \leq [12]-[25] < 3.0$ mag are mostly O-rich AGB stars with optically thick CDEs and the sources with $0.3 < [12]-[25] \leq 0.4$ mag are dominated by carbon stars. These two types of sources show different longitude distributions from each other. We estimated the distances of these two types of sources and derived the space distributions for respective groups. The principal conclusions obtained can be summarized in the following.

O-rich AGB stars are distributed with the highest stellar density at the GC and the density decreases with an increase in the *R*g. On the other hand, carbon stars show a uniform distribution projected onto the Galactic plane within about 3.6 kpc of the Sun. Thus our result suggests that the space distribution of carbon stars is different from that of O-rich AGB stars on the large scale of the Galaxy.

On the basis of these results we conclude that the ratio of carbon stars to O-rich AGB stars increases with the increase in the *R*g between about 5 and 12 kpc. This ratio is inversely correlated with the metallicity.

Acknowledgements. We are grateful to Dr. T. Mikami who offered valuable data on the absolute magnitudes for a variety of late-type stars including those before publication. We are also grateful to Dr. T. Nagata who gave suggestions for evaluating the effect of the interstellar extinction. We would like to express appreciation to Dr. K. Volk for his valuable comments which contributed to the great improvement of the paper. We are grateful to Dr. P. S. Chen for offering the identification list of IRAS sources in the GCCS2. We would like to thank Drs. T. Tsuji, O. Hashimoto, and K. Ohnaka for their encouragement and valuable discussions. We also thank Dr. S. Nishimura who gave valuable information on the stellar catalogue data compiled in National Astronomical Observatory of Japan. This work was supported by Grant-in Aids for Scientific Research (06640350, 08640338) of the Ministry of Education, Science and Culture.

References

Beichman, C. A. 1987, ARA&A, 25, 521
Blanco, V. M. 1965, in Stars and Stellar Systems, vol. 5, Galactic Structure, ed. A. Blaauw, & M. Schmidt (Chicago: Univ. Chicago Press), 241
Brewer, J. P., Richer, H. B., & Crabtree, D. R. 1995, AJ, 109, 2480
Cheeseman, P., Stutz, J., Self, M., et al. 1989, Automatic Classification of Spectra From the Infrared Astronomical Satellite (IRAS), NASA Reference Publication, 1217
Claussen, M. J., Kleinmann, S. G., Joyce, R. R., & Jura, M. 1987, ApJS, 65, 385
Groenewegem, M. A. T., de Jong, T., van der Blieck, N. S., Slijkhuis, S., & Willems, F. J. 1992, A&A, 253, 150
Guglielmo, F., Epchtein, N., Le Bertre, T., et al. 1993, A&AS, 99, 31
Habing, H. J., Olnon, F. M., Chester, T., et al. 1985, A&A, 152, L1
IRAS Science Team 1986, A&AS, 65, 607
Jura, M., & Kleinmann, S. G. 1990, ApJ, 364, 663
Mikami, T. 1975, PASJ, 27, 445
Neugebauer, G., & Leighton, R. B. 1969, Two Micron Sky Survey (NASA SP-3047)
Noguchi, K., Kawara, K., Kobayashi, Y., et al. 1981, PASJ, 33, 373
Noguchi, K., Sun, J., & Wang, G. 1991, PASJ, 43, 275
Noguchi, K., Qian, Z., Wang, G., & Wang, J. 1993, PASJ, 45, 65
Pritchet, C. J., Richer, H. B., Schade, D., Crabtree, D., & Yee, H. K. C. 1987, ApJ, 323, 79
Rieke, G. H., & Lebofsky, M. J. 1985, ApJ, 288, 618
Rolleston, W. R. J., Smartt, S. J., Dufton, P. L., & Ryans, R. S. I. 2000, A&A, 363, 537
Smartt, S. J., & Rolleston, W. R. J. 1997, ApJ, 481, L47
Stephenson, C. B. 1989, Publ. Warner Swasey Obs., 3, No. 2
Thronson, H. A., Jr., Latter, W. B., Black, J. H., Bally, J., & Hacking, P. 1987, ApJ, 322, 770
Wainscoat, R. J., Cohen, M., Volk, K., Walker, H. J., & Schwartz, D. E. 1992, ApJS, 83, 111